CONFLICT RESOLUTION FOR AIR TRAFFIC MANAGEMENT: A STUDY IN MUTLI-AGENT HYBRID SYSTEMS

by

Claire Tomlin, George J. Pappas and Shankar Sastry

CONFLICT RESOLUTION FOR AIR TRAFFIC MANAGEMENT: A STUDY IN MULTI-AGENT HYBRID SYSTEMS

by

Claire Tomlin, George J. Pappas, and Shankar Sastry

ELECTRONICS RESEARCH LABORATORY

College of Engineering
University of California, Berkeley
94720

Conflict Resolution for Air Traffic Management: a Study in Multi-Agent Hybrid Systems *

Claire Tomlin, George J. Pappas and Shankar Sastry

Department of Electrical Engineering and Computer Sciences

University of California at Berkeley

Berkeley, CA 94720

{clairet,gpappas,sastry}@eecs.berkeley.edu

Abstract

Air Traffic Management (ATM) of the future allows for the possibility of *free flight*, in which aircraft choose their own optimal routes, altitudes, and velocities. The safe resolution of trajectory conflicts between aircraft is necessary to the success of such a distributed control system. In this paper, we present a method to synthesize provably safe conflict resolution maneuvers. The method models the aircraft and the maneuver as a *hybrid control system*, and calculates the maximal set of safe initial conditions for each aircraft, so that separation is assured in the presence of uncertainties in the actions of the other aircraft. Examples of maneuvers using both speed and heading changes are worked out in detail.

Index terms: hybrid systems, air traffic management, conflict resolution, verification.

1 Introduction

Air transportation systems are faced with soaring demands for air travel. The annual air traffic rate in the U.S. is expected to grow by 3 to 5 percent annually for at least the next 15 years [1]. The current National Airspace System (NAS) architecture and management will not be able to efficiently handle this increase because of several limiting factors including:

- **Inefficient airspace utilization:** Currently, the airspace is very rigidly structured and aircraft are forced to travel along predetermined jetways. This is clearly not optimal and disallows aircraft to fly directly to the destination and take advantage of favorable winds. This problem is particularly evident in transoceanic routes which are experiencing the greatest demand growth (for example, nearly 15% [1] annually across the Pacific Ocean).

- **Increased Air Traffic Control (ATC) workload:** Separation among aircraft as well as vectoring aircraft in order to avoid weather hazards is performed centrally by ATC. In congested areas, such the regions close to urban airports referred to as TRACONs, controllers frequently simplify their heavy workload by keeping aircraft in holding patterns outside the TRACON.

- **Obsolete technology:** The computer technology used in most ATC centers is nearly 30 years old [2]. Communication is restricted to congested voice communication between the aircraft and ATC. Navigation is performed by flying over fixed VHF Omni-Directional Range (VOR) points.

In view of the above problems, the aviation community is working towards an innovative concept called *Free Flight* [3]. Free Flight allows pilots to choose their own routes, altitude and speed. User preference would be restricted only in congested airspace, or to prevent unauthorized entry of special use airspace (such as military airspace). Free Flight is potentially feasible because of enabling technologies such as Global Positioning Systems (GPS), datalink communications like Automatic Dependence Surveillance-Broadcast (ADS-B) [4, 5], Traffic Alert and Collision Avoidance Systems (TCAS) [6] and powerful on-board computation. In addition, tools such as NASA's Center-TRACON Automation System (CTAS) [7] and MITRE's URET [8] will serve as decision support tools for ground controllers in an effort to reduce ATC workload and optimize capacity.

The above technological advances will also enable the current ATC system to accommodate future air traffic growth: sophisticated on-board equipment will allow aircraft to share some of the workload, such as navigation, weather prediction and aircraft separation, with ground controllers. In order to improve the current standards of safety in an unstructured, Free Flight environment, conflict detection and resolution algorithms are vital. Such algorithms would be used either on the ground by Air Traffic Control or in the air by the Flight Management System (FMS) of each aircraft.

In the proposed Free Flight airspace, each aircraft is surrounded by two virtual *cylinders* [4], the *protected zone* and the *alert zone*, shown in Figure 1. A conflict or loss of separation between two aircraft occurs whenever the protected zones of the aircraft overlap. The radius and the height of the en-route protected zone over U.S. airspace is currently 2.5 nautical miles and 2,000 ft
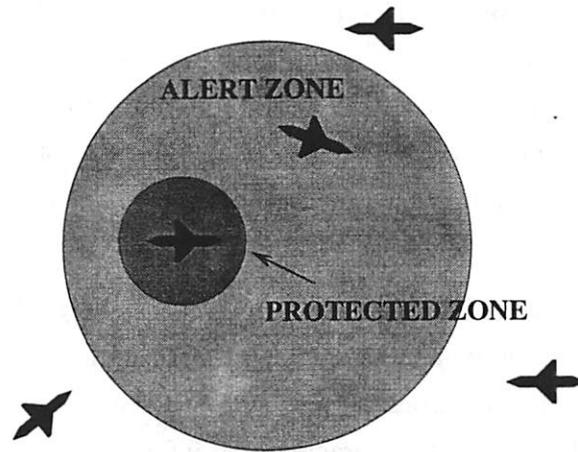
Figure 1: Aircraft Zones

(1, 000 ft below 29, 000 ft, 4, 000 ft over oceanic airspace) respectively. The size of the alert zone, currently under debate, depends on various factors including airspeed, altitude, accuracy of sensing equipment, traffic situation, aircraft performance and average human and system response times. When an aircraft enters the alert zone of another aircraft, the aircraft exchange sensor and intent information in order to predict and resolve the conflict.

Current research endeavors in conflict prediction and resolution include [9, 10, 11, 12, 13]. Conflict prediction could be spatial, temporal or probabilistic. Spatial and temporal approaches, such as [11, 13], calculate the four dimensional coordinates of a possible conflict. Probabilistic approaches, such as [9, 10], assume stochastic uncertainty in the measured information and determine the probability of collision. The work of [11, 12] formulates conflict resolution as an optimal control problem whereas [13] treats the problem as a convex optimization problem. The user interface of CTAS allows controllers to manually alter aircraft trajectories to resolve conflicts in en route airspace [14]. TCAS [6] provides resolution advisories (flight level changes) to pilots involved in two-aircraft conflicts, however these advisories are not formally verified. Conflict prediction, resolution, and verification are the most important modules that are in need of augmentation in the current implementations of CTAS and TCAS.

In [15] a possible future architecture for Air Traffic Management (ATM) is presented. In our paradigm, aircraft are allowed to self-optimize in the spirit of Free Flight, communicate state and intent data to each other using an ADS-B datalink for conflict prediction, and coordinate with each other to resolve potential conflicts. State and intent data could be uncertain. Coordination among the aircraft is in the form of *maneuvers* which are finite sequences of *flight modes* such as heading, altitude and speed changes for each aircraft. These types of maneuvers are routinely used in current Air Traffic Control practice since they are easily understandable by pilots as well as easily

3

implementable by on-board autopilots which regulate the aircraft to heading and speed setpoints. The main thrust of our conflict resolution algorithms is to *verify* that a maneuver successfully resolves the conflict by computing the set of initial conditions for which the maneuver is safe, where safety means that separation is maintained. In the presence of bounded uncertainty in the state or intent data, we take a worst-case approach and verify that the worst-case system trajectory is safe.

The flight mode switching occurring in each maneuver is modeled by a finite state automaton with the relative aircraft configuration dynamics residing within each flight mode. A conflict resolution maneuver is therefore modeled by a finite state automaton interacting with a set of control systems, resulting in a *hybrid control system*. The interaction and information exchange of all of the aircraft involved in the maneuver results in a *multi-agent hybrid control system*.

There are several approaches to hybrid system modeling, verification, and controller design (see, for example, [16, 17, 18, 19]). The computer science approach is to extend models of finite state automata to timed automata [20], linear hybrid automata [21], and hybrid input/output automata [22]. Linear hybrid automata model or abstract the continuous dynamics by differential inclusions of the form $A\dot{x} \leq b$ and verify properties of the resulting abstracted system [23, 24, 25]. Specifications are verified for these models using either model checking, which exhaustively check all system trajectories, or deductive theorem proving techniques [26], which prove the specification by induction on all system trajectories. In this framework, controller design has also been developed [27, 28]. Automated computational tools have been developed for both model checking [29, 30], and theorem proving [31]. Control theoretic approaches to modeling, analysis, and controller design for hybrid systems have extended the theory of dynamical systems to include discrete modes of operation. Modeling approaches include those of [32, 33, 34, 35, 36, 37]. Analysis and design techniques extend existing control techniques, such as stability theory [33], optimal control [33, 36, 37], and control of discrete event systems [38, 39], to hybrid systems.

Our conflict resolution algorithms are in the spirit of model checking, but we use control theoretic (deductive) techniques to calculate the reachable region for hybrid systems with general nonlinear dynamics. Our method calculates the largest controlled invariant subset of the complement of each aircraft's protected zone, taking into account the uncertainty of the actions of the other aircraft. In order to compute this safe set of initial states, we first develop a method to compute the controlled invariant subsets for continuous systems in the presence of disturbances. A natural framework for this type of problem is zero-sum noncooperative dynamic game theory [40, 41]. In this framework, uncertain information about neighboring aircraft is treated as a disturbance. For a two-aircraft example, assuming a saddle solution to the game exists, each aircraft chooses an optimal policy assuming the worst possible disturbance. This is motivated by the work of [42], in which game

4

theoretic methods are used to prove safety of a set of maneuvers in Intelligent Vehicle Highway Systems.

Along with the safe set of initial states, we calculate the corresponding safe set of control inputs as a function of the state. Within its safe region of operation, the aircraft may design its trajectory to optimize over other criteria, such as fuel efficiency or minimal deviation from route. At the boundary of its safe region, the aircraft must apply the particular control which keeps it out of its unsafe region. Thus, we are naturally led to a switching control based protocol which is *least restrictive*. A more detailed description of this multiobjective methodology may be found in [43]. The resultant hybrid system is safe by design, as we illustrate with two versions of an interesting example of two aircraft conflict resolution in the horizontal plane.

The organization of this paper is as follows: In Section 2 our modeling formalism and design methodology for hybrid systems is described. Section 3 presents the game theoretic approach to computing the safe set of initial conditions and control inputs for continuous systems. Section 4 describes safety verification of coordinated maneuvers using the results of Section 3. Section 5 presents a brief summary and some issues for further research.

2   Hybrid Model and Design Methodology

In this section, we present a hybrid system model for conflict resolution maneuvers, and a method to verify the safety of, and synthesize control schemes for these maneuvers. The discrete states of the hybrid system model the different flight modes that each aircraft steps through while executing the maneuver. For example, consider the two-aircraft examples of Figure 2. In the first, the aircraft avoid each other by transitioning through a sequence of heading changes: "left", "straight", "right", and then back to the original "cruise" mode; in the second the conflict is avoided by both aircraft transitioning to a "circle" mode from a "cruise" mode.

Each mode has associated with it the relative aircraft configuration dynamics. The verification of the safety of each maneuver, with possible variations in the control inputs of each aircraft and changes in the switching times between modes, is complicated and in general not possible to compute manually. The hybrid model presented in this section provides an organized, formal way to model and prove the safety of the maneuver.

The hybrid model described below is inspired by that of [23] for linear hybrid automata, with the difference that we allow for a nonlinear continuous dynamic model within each discrete state and a general discrete transition relation.
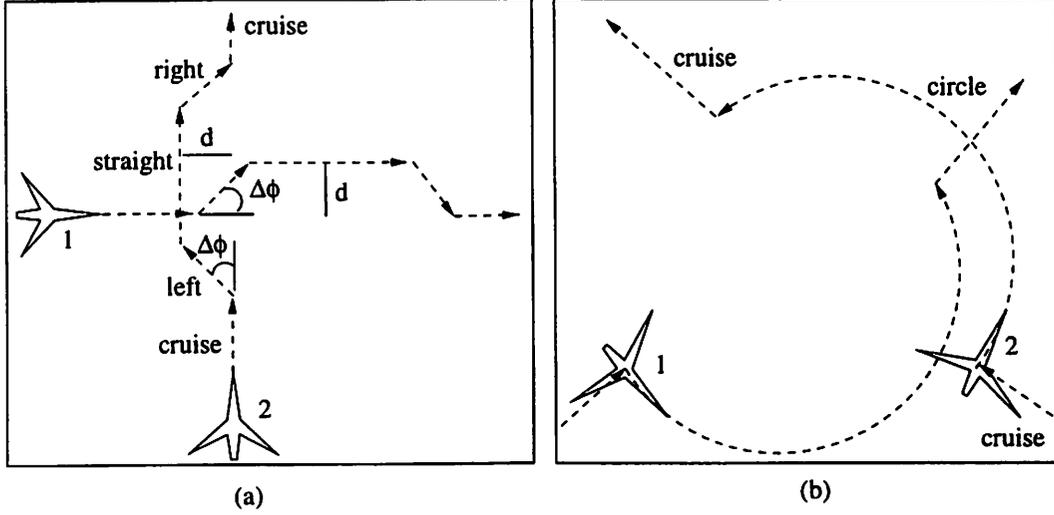
Figure 2: Two different conflict resolution maneuvers, with associated modes.

Hybrid System Model

A hybrid system H is defined to be the tuple $H = (Q \times M, U \times D, \Sigma, I, Inv, E, f)$, in which:

- $Q \times M$ is the state space, with $Q = \{q_1, q_2, \ldots, q_m\}$ a finite set of discrete states, and M an n-manifold; a state of the system is a pair $(q_i, x) \in Q \times M$;

- $U \times D \subset \mathbb{R}^u \times \mathbb{R}^d$ is the product of the input set and disturbance set; the space of acceptable control and disturbance trajectories are denoted by $\mathcal{U} = \{u(\cdot) \in PC^0 | u(\tau) \in U \; \forall \tau \in \mathbb{R}\}$, $\mathcal{D} = \{d(\cdot) \in PC^0 | d(\tau) \in D \; \forall \tau \in \mathbb{R}\}$;

- Σ is a finite set of transition labels;

- $I \subset Q \times M$ is the set of initial conditions;

- $Inv : Q \to 2^M$ is the invariant associated with each discrete state, meaning that the state (q, x) may flow within q only if $x \in Inv(q)$;

- $E \subset Q \times M \times \Sigma \times Q \times M$ is the set of discrete jumps with $(q, x, \sigma, q', x') \in E$ meaning that if the current state is (q, x), the system may instantaneously take a discrete transition σ to state (q', x');

- $f : Q \times M \times U \times D \to TM$ is a map which associates with each discrete state $q \in Q$ a control system $f(q, x, u, d)$. For notational convenience we use $f_q(x, u, d)$ to denote $f(q, x, u, d)$.

Hybrid systems evolve in so-called "dense time" by either continuous flows or discrete transitions. Trajectories of the hybrid system H starting at a state (q, x) evolve according to $f_q(\cdot)$ as long as the

6

continuous state remains within $Inv(q)$. If the invariance condition is not satisfied then a discrete transition is forced and the continuous state may be reinitialized. If $(q, x, \sigma, q', x') \in E$ then the discrete state may jump from q to q' and the continuous state x is reinitialized to x' and then flows according to $f_{q'}(\cdot)$.

Relative Aircraft Configuration Models

We now describe the continuous dynamics within each discrete state q. Because conflicts between aircraft depend on the relative position and velocity of the agents, the continuous models we use are *relative* models, describing the motion of each aircraft in the system with respect to the other aircraft. For example, to study pairwise conflict between the trajectories of two aircraft, aircraft 1 and aircraft 2, a relative model with its origin centered on aircraft 1 is used. The configuration of an individual aircraft is described by an element of the Lie group G of rigid motions in $\mathbb{R}^2$ or $\mathbb{R}^3$, called $SE(2)$ or $SE(3)$ respectively. In planar situations, in which aircraft are flying at the same altitude, $SE(2)$ will be used.

Following the example described above, let $g_1 \in G$ denote the configuration of aircraft 1, and let $g_2 \in G$ denote the configuration of aircraft 2. The trajectories of both aircraft are kinematically modeled as left invariant vector fields on G. Therefore

$$\dot{g}_1 = g_1 X_1 \tag{1}$$

$$\dot{g}_2 = g_2 X_2 \tag{2}$$

where $X_1, X_2 \in \mathcal{G}$, the Lie algebra associated with the Lie group G. A coordinate change is performed to place the identity element of the Lie group G on aircraft 1. Thus, let $g_r \in G$ denote the relative configuration of aircraft 2 with respect to aircraft 1. Then

$$g_2 = g_1 g_r \Rightarrow g_r = g_1^{-1} g_2 \tag{3}$$

Differentiation yields the dynamics of the relative configuration,

$$\dot{g}_r = g_r X_2 - X_1 g_r \tag{4}$$

Note that the vector field which describes the evolution of g_r is neither left nor right invariant.

Consider the Lie group $SE(2)$ and its associated Lie algebra $se(2)$. A coordinate chart for $SE(2)$ is given by x, y, ϕ representing the planar position and orientation of a rigid body. In this coordinate chart, the relative configuration g_r is given in homogeneous coordinates by

$$g_r = \begin{bmatrix} \cos \phi_r & -\sin \phi_r & x_r \\ \sin \phi_r & \cos \phi_r & y_r \\ 0 & 0 & 1 \end{bmatrix} \tag{5}$$
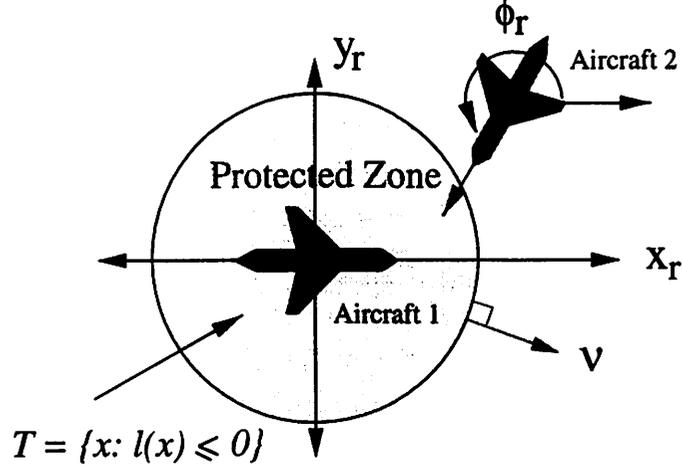
7

Figure 3: The relative configuration, showing the protected zone and outward pointing normal.

where x_r, y_r represent the relative position of aircraft 2 with respect to aircraft 1 and ϕ_r is the relative orientation. In local coordinates, the coordinate transformation (3) is expressed as

$$\begin{bmatrix} x_r \\ y_r \end{bmatrix} = R(-\phi_1) \begin{bmatrix} x_2 - x_1 \\ y_2 - y_1 \end{bmatrix} = \begin{bmatrix} \cos(-\phi_1) & -\sin(-\phi_1) \\ \sin(-\phi_1) & \cos(-\phi_1) \end{bmatrix} \begin{bmatrix} x_2 - x_1 \\ y_2 - y_1 \end{bmatrix} \tag{6}$$

$$\phi_r = \phi_2 - \phi_1 \tag{7}$$

with x_i, y_i, ϕ_i parameterizing the absolute position and orientation of aircraft i. The Lie algebra elements $X_1, X_2 \in se(2)$ are represented as matrices in $\mathbb{R}^{3 \times 3}$ of the form

$$X_1 = \begin{bmatrix} 0 & -\omega_1 & v_1 \\ \omega_1 & 0 & 0 \\ 0 & 0 & 0 \end{bmatrix} \qquad X_2 = \begin{bmatrix} 0 & -\omega_2 & v_2 \\ \omega_2 & 0 & 0 \\ 0 & 0 & 0 \end{bmatrix} \tag{8}$$

where v_i, ω_i represent the linear and angular velocities. Inserting equations (5) and (8) in equation (4) results in the $SE(2)$ relative configuration dynamics in local coordinates

$$\dot{x}_r = -v_1 + v_2 \cos \phi_r + \omega_1 y_r$$

$$\dot{y}_r = v_2 \sin \phi_r - \omega_1 x_r \tag{9}$$

$$\dot{\phi}_r = \omega_2 - \omega_1$$

Similar results for $SE(3)$ may be found in [44]. Thus for each discrete state q, the dynamics $\dot{x} = f_q(x, u, d)$ is described by (9), with $x = (x_r, y_r, \phi_r)^T$. The linear (or angular) velocity of aircraft 1 is the control input u, and the uncertain linear (or angular) velocity of aircraft 2 is considered to be the disturbance d.

8

Design and Verification Methodology

In the remainder of this paper we derive a method to generate the unsafe region of the state space $Q \times M$, which is the subset of initial states I for which, regardless of the control input, there exists a trajectory of H from this subset to an illegal region of the state space.

Given a subset $K \subset Q \times M$, we define the predecessor of K under continuous flows as

$$
\begin{aligned}
Pre_t(K) = \quad & \{(q,x) \in Q \times M \mid \exists (q',x') \in K \text{ such that } q' = q \text{ and} \\
& \exists d(\cdot) \in \mathcal{D}, \forall u(\cdot) \in \mathcal{U}, \text{ and } x(\tau) \in Inv(q), \forall \tau \in [t,0], \text{ satisfying} \\
& x(t) = x, x(0) = x', \text{ and } \dot{x}(\tau) = f_q(x(\tau), u(\tau), d(\tau))\}
\end{aligned}
\tag{10}
$$

Similarly, the predecessor of K under discrete transitions $\sigma \in \Sigma$ is defined to be

$$
Pre_\sigma(K) = \{(q,x) \in Q \times M \mid \exists (q',x') \in K \text{ and } (q,x,\sigma,q',x') \in E\}
\tag{11}
$$

The predecessor under continuous flows or discrete transitions is defined as

$$
Pre(K) = \left(\bigcup_{\sigma \in \Sigma} Pre_\sigma(K) \right) \cup Pre_{-\infty}(K)
\tag{12}
$$

The unsafe region of the state space will be computed by recursively applying this $Pre(K)$ operator:

$$
\begin{aligned}
Pre^2(K) &= Pre(Pre(K)) \\
&\vdots \\
Pre^n(K) &= Pre(Pre^{n-1}(K)) \\
&\vdots
\end{aligned}
\tag{13}
$$

A fixed point of this iteration, if it exists, is denoted $Pre^*(K)$, ie. $Pre^*(K) = Pre(Pre^*(K))$.

For two aircraft conflicts, we define the illegal region to be the *relative* protected zone, or the 5-mile radius cylinder around aircraft 1, denoted T with boundary ∂T, illustrated in Figure 3. In Section 3, a methodology is developed to compute $Pre_t(T)$, using level sets of an appropriate Hamilton-Jacobi-Isaacs partial differential equation. This computation is subsequently used in Section 4 to verify the conflict resolution maneuver.

3 The Hamilton-Jacobi-Isaacs Approach for Continuous Systems

Consider the dynamics of the aircraft in one discrete state $q \in Q$ (for notational simplicity we drop the subscript q in this section):

$$
\dot{x} = f(x,u,d) \qquad x(t) = x
\tag{14}
$$

where $x \in \mathbb{R}^n$ describes the relative configuration of aircraft 2 with respect to aircraft 1, $u \in U \subset \mathbb{R}^u$ is the control input which models the actions of aircraft 1, and $d \in D \subset \mathbb{R}^d$ is the disturbance input which models the actions of aircraft 2. We assume that the system starts at state x at initial time t. Both U and D are known sets, but whereas the control input u may be chosen by the designer, the disturbance d is unknown, and models the uncertainty of the actions of aircraft 2.

The goal is to maintain safe operation of the system (14), meaning that the system trajectories do not enter T, the "Target set". We assume that there exists a differentiable function $l(x)$ so that $T = \{x \in \mathbb{R}^n \mid l(x) \le 0\}$ and $\partial T = \{x \in \mathbb{R}^n \mid l(x) = 0\}$.

3.1   The Value Function and the Hamilton-Jacobi-Isaacs Equation

This section describes the computation of the unsafe subset of the state space, denoted $Pre_t(T) \subset M$, which is the subset of initial states of (14) from which there exists a disturbance action $d(\cdot)$ such that the resulting trajectory of (14) enters T in at most t seconds. Due to the uncertainty in the actions of aircraft 2, the safest possible strategy of aircraft 1 is to fly a trajectory which guarantees that the minimum allowable separation with aircraft 2 is maintained, *regardless* of the actions of aircraft 2. We formulate this problem as a two-person, zero-sum dynamical game, and calculate the "losing" states for aircraft 1.

Consider the system (14) over the time interval $[t, 0]$, where $t < 0$. The value function of the game is defined by:

$$J(x, u(\cdot), d(\cdot), t) : \mathbb{R}^n \times \mathcal{U} \times \mathcal{D} \times \mathbb{R}_- \to \mathbb{R} \tag{15}$$

such that $J(x, u(\cdot), d(\cdot), t) = l(x(0))$. This value function may be interpreted as the cost of a trajectory $x(\cdot)$ which starts at x at time $t \le 0$, evolves according to (14) with input $(u(\cdot), d(\cdot))$, and ends at the final state $x(0)$. Note that the value function depends only on the final state: there is no running cost, or *Lagrangian*. This encodes the fact that we are only interested in whether or not the system trajectory ends in T and are not concerned with intermediate states. The game is won by aircraft 1 if the terminal state $x(0)$ is either outside T or on ∂T (i.e. $J(x, 0) \ge 0$), and is won by aircraft 2 otherwise.

Given $J(x, u(\cdot), d(\cdot), t)$, we first characterize the *unsafe* portion of ∂T, defined as those states $x \in \partial T$ for which there exists some disturbance $d \in D$ such that for all inputs $u \in U$ the vector field points into T; the *safe* portion of ∂T consists of the states $x \in \partial T$ for which there is some input $u \in U$ such that for all disturbances $d \in D$, the vector field points outward from T. Define the outward pointing normal to T as $\nu = Dl(x)$, then

$$
\begin{aligned}
&\text{Safe portion of } \partial T &&\{x \in \partial T : \exists u \forall d \quad \nu^T f(x, u, d) \ge 0\} \\
&\text{Unsafe portion of } \partial T &&\{x \in \partial T : \forall u \exists d \quad \nu^T f(x, u, d) < 0\}
\end{aligned}
\tag{16}
$$

Thus, the optimal control u^* and the worst disturbance d^* are given by:

$$u^* = \arg\max_{u \in \mathcal{U}} \min_{d \in \mathcal{D}} J(x, u(\cdot), d(\cdot), t) \qquad (17)$$

$$d^* = \arg\min_{d \in \mathcal{D}} \max_{u \in \mathcal{U}} J(x, u(\cdot), d(\cdot), t) \qquad (18)$$

The game is said to have a saddle solution (u^*, d^*) if the resulting optimal cost does not depend on the order in which the maximization and minimization is performed:

$$J^*(x, t) = \max_{u \in \mathcal{U}} \min_{d \in \mathcal{D}} J(x, u(\cdot), d(\cdot), t) = \min_{d \in \mathcal{D}} \max_{u \in \mathcal{U}} J(x, u(\cdot), d(\cdot), t) \qquad (19)$$

The concept of a saddle solution is key to our computation of the safe regions of operation of the aircraft, since a solution of (14) with $u = u^*$ and $d = d^*$ represents an optimal trajectory for *each* player under the assumption that the other player plays its optimal strategy.

Aircraft 1 maintains safety at time t by operating outside of $Pre_t(T)$:

$$Pre_t(T) = \{x \in Inv(q) \mid \exists d(\cdot) \in \mathcal{D}, J(x, u(\cdot), d(\cdot), \tau) < 0, \forall u(\cdot) \in \mathcal{U}, \forall \tau \in [t, 0]\} \qquad (20)$$

$$= \{x \in M \mid \exists d(\cdot) \in \mathcal{D}, J(x, u^*(\cdot), d(\cdot), \tau) < 0, \forall \tau \in [t, 0]\} \bigcap Inv(q) \qquad (21)$$

Let $\partial Pre_t(T)$ denote the boundary of $Pre_t(T)$. To calculate the unsafe set of states for all $t \in (-\infty, 0]$, we construct the Hamilton-Jacobi-Isaacs partial differential equation for this system and attempt to calculate its steady state solution. Define the Hamiltonian $H(x, p, u, d) = p^T f(x, u, d)$ where $p \in T^* \mathbb{R}^n$ is the costate. The optimal Hamiltonian is given by:

$$H^*(x, p) = \max_{u \in U} \min_{d \in D} H(x, p, u, d) = H(x, p, u^*, d^*) \qquad (22)$$

and satisfies Hamilton's equations (provided $H^*(x, p)$ is smooth in x and p):

$$\begin{aligned} \dot{x} &= \frac{\partial H^*}{\partial p}(x, p) \\ \dot{p} &= -\frac{\partial H^*}{\partial x}(x, p) \end{aligned} \qquad (23)$$

with the boundary conditions $p(0) = Dl(\dot{x}(0))$ and $x(t) = x$. If $J^*(x, t)$ is a smooth function of x and t, then $J^*(x, t)$ satisfies the Hamilton-Jacobi-Isaacs equation:

$$-\frac{\partial J^*(x, t)}{\partial t} = H^*(x, \frac{\partial J^*(x, t)}{\partial x}) \qquad (24)$$

with boundary condition $J^*(x, 0) = l(x)$. It is difficult to guarantee that the PDE (24) has smooth solutions for all $t \leq 0$, due to the occurrence of "shocks", ie. discontinuities in J as a function of x. If there are no shocks in the solution of (24), we characterize the set

$$Pre_{-\infty}(T) = \{x \in Inv(q) \mid J^*(x, \tau) < 0, \forall \tau \in (-\infty, 0]\} \qquad (25)$$

by solving the modified Hamilton-Jacobi-Isaacs equation:

$$-\frac{\partial J^*(x, t)}{\partial t} = \min\{0, H^*(x, \frac{\partial J^*(x, t)}{\partial x})\} \qquad (26)$$

11

with boundary condition $J^*(x,0) = l(x)$. The "min" is added to the right hand side of equation (26) to ensure that states which are once unsafe cannot become safe. In practical applications, since one is concerned only with aircraft in the alert zone, the calculation of equation (25) may be approximated by computing $Pre_t(T)$, for sufficiently large t, such as $t = 20$ minutes.

The set $Pre_{-\infty}(T)$ defines the *least restrictive control scheme* for safety. If aircraft 2 is outside $Pre_{-\infty}(T)$, any control input may be safely applied by aircraft 1, whereas on the boundary, the only input which may be safely applied to ensure safety is u^*. The safe set of control inputs associated with each state at time t is

$$\mathcal{U}_s(x,t) = \{u \in \mathcal{U} \mid J(x,u(\cdot),d^*(\cdot),t) \geq 0\} \qquad (27)$$

Additional system requirements, such as optimal fuel trajectories and passenger comfort, can now be incorporated by optimizing secondary and tertiary criteria within the constraints of set (27), following the multiobjective design methodology of [43].

We now apply this general framework to the planar $SE(2)$ relative model (9) in local coordinates (x_r, y_r, ϕ_r), with the control actions either the angular or linear velocities.

3.2 Angular Velocities as Control Actions

Consider the case in which the linear velocities of both aircraft are fixed, $v_1, v_2 \in \mathbb{R}$, and the control inputs of the aircraft are the angular velocities, $u = \omega_1$ and $d = \omega_2$:

$$
\begin{aligned}
\dot{x}_r &= -v_1 + v_2 \cos\phi_r + uy_r \\
\dot{y}_r &= v_2 \sin\phi_r - ux_r \\
\dot{\phi}_r &= d - u
\end{aligned}
\qquad (28)
$$

with state variables $x_r, y_r \in \mathbb{R}$, $\phi_r \in [-\pi, \pi)$, and control and disturbance inputs $u \in \mathcal{U} = [\underline{\omega}_1, \overline{\omega}_1] \subset \mathbb{R}$, $d \in \mathcal{D} = [\underline{\omega}_2, \overline{\omega}_2] \subset \mathbb{R}$. Without loss of generality (we scale the coefficients of u and d if this is not met), assume that $\underline{\omega}_i = -1$ and $\overline{\omega}_i = 1$, for $i = 1, 2$.

The target set T is the protected zone in the relative frame:

$$T = \{(x_r, y_r) \in \mathbb{R}^2, \phi_r \in [-\pi, \pi) \mid x_r^2 + y_r^2 \leq 5^2\} \qquad (29)$$

which is a 5-mile-radius cylindrical block in the (x_r, y_r, ϕ_r) space. Thus the function $l(x)$ may be defined as

$$l(x) = x_r^2 + y_r^2 - 5^2 \qquad (30)$$

The optimal Hamiltonian is

$$H^*(x,p) = \max_{u \in U} \min_{d \in D} [-p_1 v_1 + p_1 v_2 \cos\phi_r + p_2 v_2 \sin\phi_r + (p_1 y_r - p_2 x_r - p_3)u + p_3 d] \qquad (31)$$

Defining the *switching functions* $s_1(t)$ and $s_2(t)$, as

$$
\begin{aligned}
s_1(t) &= p_1(t)y_r(t) - p_2(t)x_r(t) - p_3(t) \\
s_2(t) &= p_3(t)
\end{aligned}
\tag{32}
$$

the saddle solution u^*, d^* exists when $s_1 \neq 0$ and $s_2 \neq 0$ and are calculated as

$$
\begin{aligned}
u^* &= sgn(s_1) \\
d^* &= -sgn(s_2)
\end{aligned}
\tag{33}
$$

The equations for $\dot{p}$ are obtained through (23) and are

$$
\begin{aligned}
\dot{p}_1 &= u^* p_2 \\
\dot{p}_2 &= -u^* p_1 \\
\dot{p}_3 &= p_1 v_2 \sin \phi_r - p_2 v_2 \cos \phi_r
\end{aligned}
\tag{34}
$$

with $p(0) = (x_r, y_r, 0)^T = \nu$, the outward-pointing normal to ∂T at any point (x_r, y_r, ϕ_r) on ∂T.

The safe and unsafe portions of ∂T are calculated using equations (16) with $\nu = (x_r, y_r, 0)^T$. Thus, those (x_r, y_r, ϕ_r) on ∂T for which

$$
- v_1 x_r + v_2(x_r \cos \phi_r + y_r \sin \phi_r) < 0
\tag{35}
$$

constitute the unsafe portion, and those (x_r, y_r, ϕ_r) on ∂T for which

$$
- v_1 x_r + v_2(x_r \cos \phi_r + y_r \sin \phi_r) = 0
\tag{36}
$$

are the final state conditions for the boundary of the unsafe set $Pre_t(T)$. To solve for $p(t)$ and $x(t)$ along this boundary for $t < 0$, we must first determine $u^*(0)$ and $d^*(0)$. Equations (33) are not defined at $t = 0$, since $s_1 = s_2 = 0$ on ∂T, giving rise to "abnormal extremals" (meaning that the optimal Hamiltonian loses dependence on u and d at these points. Analogously to [41] (p. 442-443), we use an indirect method to calculate $u^*(0)$ and $d^*(0)$: at any point (x_r, y_r, ϕ_r) on ∂T, the derivatives of the switching functions s_1 and s_2 are

$$
\dot{s}_1 = y_r v_1
\tag{37}
$$

$$
\dot{s}_2 = x_r v_2 \sin \phi_r - y_r v_2 \cos \phi_r
\tag{38}
$$

For points $(x_r, y_r, \phi_r) \in \partial T$ such that $\phi_r \in (0, \pi)$ it is straightforward to show that $\dot{s}_1 > 0$ and $\dot{s}_2 > 0$, meaning that for values of t slightly less than 0, $s_1 < 0$ and $s_2 < 0$. Thus for this range of points along ∂T, $u^*(0) = -1$ and $d^*(0) = 1$. These values for u^* and d^* remain valid for $t < 0$ as long as $s_1(t) < 0$ and $s_2(t) < 0$. When $s_1(t) = 0$ and $s_2(t) = 0$, the saddle solution switches and the computation of the boundary continues with the new values of u^* and d^*, thus introducing "kinks" into the boundary. These points correspond to loss of smoothness in the Hamilton-Jacobi-Isaacs
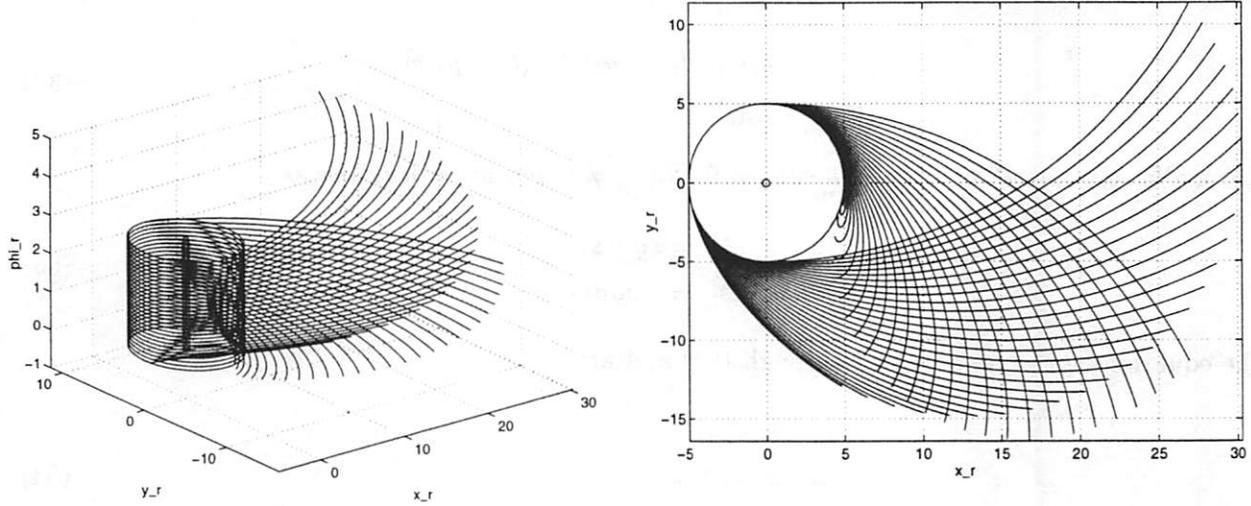
Figure 4: The Target set $T = \{(x_r, y_r), \phi_r \in (0, \pi) \mid x_r^2 + y_r^2 \le 5^2\}$ (cylinder) and the boundary of the set $Pre_t(T)$ (enclosed by the boundary) for $t < 0$ until the first switch in either $s_1(t)$ or $s_2(t)$. The second picture is a top view of the first.

equation discussed above. Figure 4 displays the resulting boundary of the unsafe set $Pre_t(T)$, for $t < 0$ until the first time that either $s_1(t)$ or $s_2(t)$ switches.

The automaton illustrating the *least restrictive control scheme* for safety is shown in Figure 5. The computation of the boundary of $Pre_{-\infty}(T)$ is in general difficult. For certain ranges of $\mathcal{U}$ and $\mathcal{D}$, the surfaces shown in Figure 4 intersect, and at the intersection, it is not clear that u^* is the unique safe input.

3.3 Linear Velocities as Control Actions

Now consider the case in which the angular velocities of the two aircraft are zero, and the control inputs are the linear velocities of the aircraft: $u = v_1$, $d = v_2$, and model (9) reduces to:

$$
\begin{aligned}
\dot{x}_r &= -u + d \cos \phi_r \\
\dot{y}_r &= d \sin \phi_r \\
\dot{\phi}_r &= 0
\end{aligned}
\tag{39}
$$

The input and disturbance lie in closed subsets of the positive real line $u \in \mathcal{U} = [\underline{v}_1, \overline{v}_1] \subset \mathbb{R}^+$, $d \in \mathcal{D} = [\underline{v}_2, \overline{v}_2] \subset \mathbb{R}^+$.

The Target set T and function $l(x)$ are defined as in the previous example. In this example, it is straightforward to calculate the saddle solution (u^*, d^*) directly, by integrating equations (39) for

14

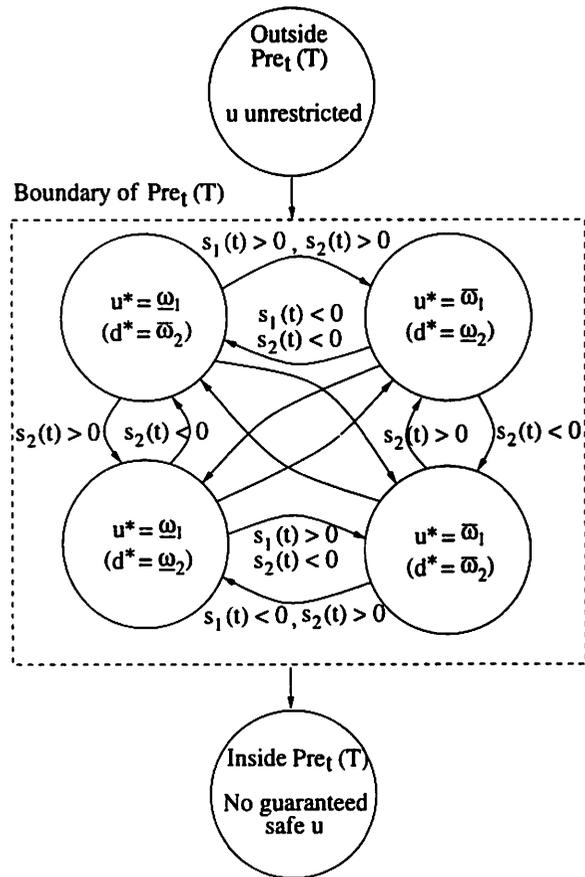Figure 5: Switching law governing the two aircraft system with angular velocity control inputs. The law is least restrictive in that the control u is not restricted when the state is outside $Pre_t(T)$. The diagonal transitions in the automaton for the boundary of $Pre_t(T)$ are not labeled for legibility. In practice, t should be chosen large enough to take into account aircraft in the alert zone.

piecewise constant u and d, and substituting the solutions into the cost function (15). To do this we first define the switching functions s_1 and s_2 as

$$
\begin{aligned}
s_1(t) &= x_r \\
s_2(t) &= x_r \cos \phi_r + y_r \sin \phi_r
\end{aligned}
\tag{40}
$$

Proposition 1 [Saddle Solution for Linear Velocity Controls] *The global saddle solution (u^*, d^*) to the game described by system (39) for the cost $J(x, u(\cdot), d(\cdot), t)$ given by equation (15) is*

$$
u^* = \begin{cases} \underline{v}_1 & \text{if } sgn(s_1) > 0 \\ \overline{v}_1 & \text{if } sgn(s_1) < 0 \end{cases}
\tag{41}
$$

$$
d^* = \begin{cases} \underline{v}_2 & \text{if } sgn(s_2) > 0 \\ \overline{v}_2 & \text{if } sgn(s_2) < 0 \end{cases}
\tag{42}
$$

Proof: In Appendix. □

As can be seen from equation (41), u^* depends on the position of aircraft 2 relative to aircraft 1. If aircraft 2 is ahead of aircraft 1 in the relative axis frame, then u^* is at its lower limit, if aircraft 2 is behind aircraft 1 in the relative axis frame then u^* is at its upper limit. If aircraft 2 is heading towards aircraft 1, then d^* is at its upper limit, if aircraft 2 is heading away from aircraft 1, d^* is at its lower limit. The bang-bang nature of the saddle solution allows us to abstract the system behavior by the hybrid automaton shown in Figure 6, which describes the least restrictive control scheme for safety. The unsafe sets of states are illustrated in Figure 7 for various values of ϕ_r, and speed ranges as illustrated.

4. Verification of Conflict Resolution Maneuvers

In this section we apply the $Pre_t(T)$ calculation of Section 3 to calculate the unsafe set of initial conditions for a conflict resolution maneuver. We illustrate the methodology on a maneuver whose form is chosen to be a finite sequence of heading changes resulting in a trapezoidal deviation from the desired path. Consider the conflict scenario and resolution maneuver shown in Figure 2 (a). The protocol may be linguistically expressed as follows:

1. Cruise until aircraft are α_1 miles apart;

2. Make a heading change of $\Delta \phi$ and fly until a lateral displacement of at least d miles is achieved for both aircraft;

3. Make a heading change to original heading and fly until the aircraft are α_2 miles apart;
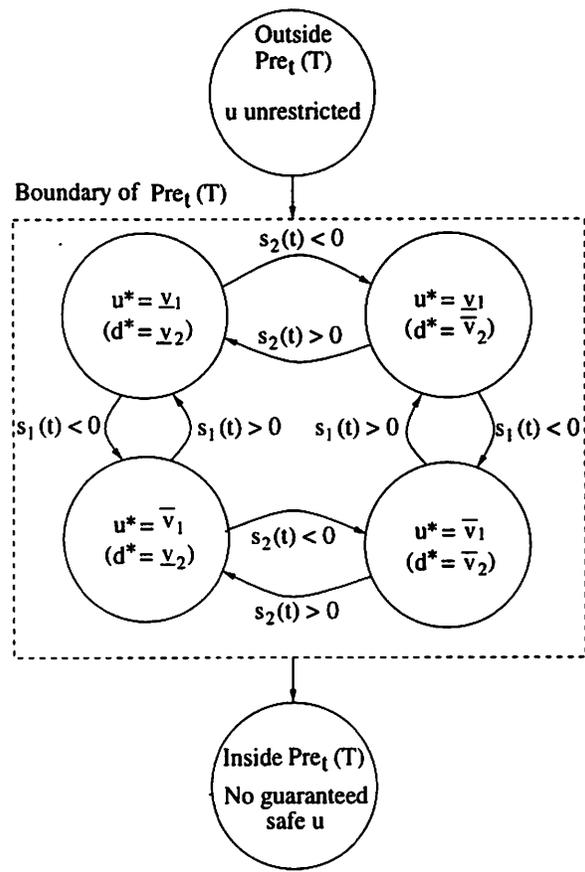
16

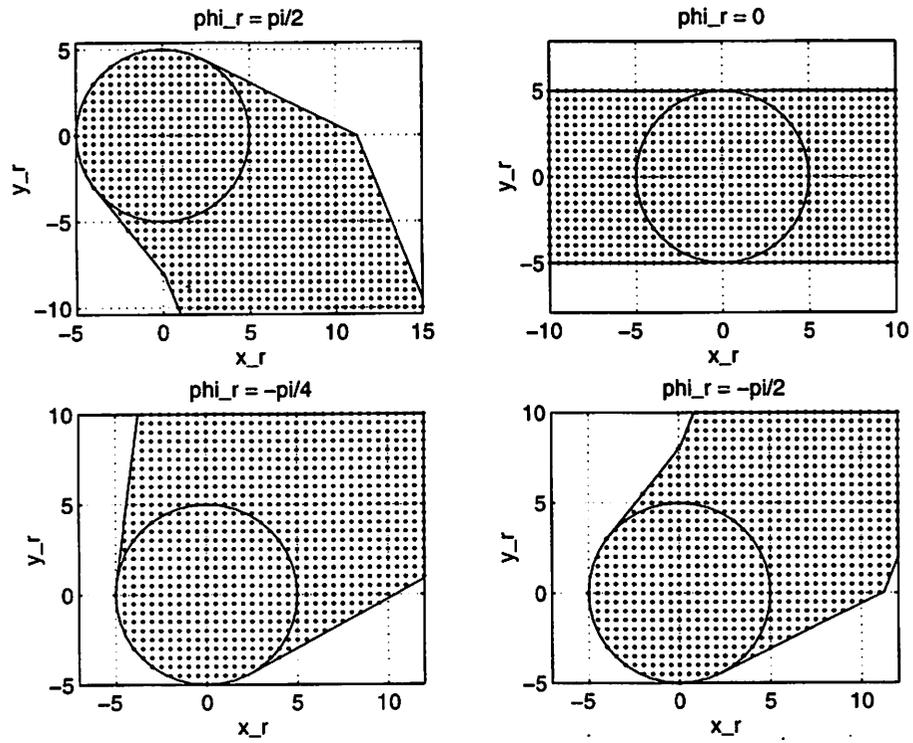Figure 6: Switching law governing the two aircraft system with linear velocity control inputs.

Figure 7: $Pre_t(T)$ shown in the (x_r, y_r)-plane for $[\underline{v}_1, \overline{v}_1] = [2, 4]$, $[\underline{v}_2, \overline{v}_2] = [1, 5]$ and $\phi_r = \pi/2, 0, -\pi/4, -\pi/2$.

4. Make a heading change of $-\Delta\phi$ and fly until a lateral displacement of d miles is achieved for both aircraft;

5. Make a heading change to original heading and cruise.

The maneuver is modeled as the hybrid automaton H shown in Figure 8. The state space of H is $Q \times \mathbb{R}^2 \times S^1$ where $Q = \{CRUISE, LEFT, STRAIGHT, RIGHT\}$ and models the different flight modes in the maneuver, and $(x_r, y_r, \phi_r) \in \mathbb{R}^2 \times S^1$ are the continuous variables which evolve within each discrete location according to the relative configuration dynamics (9). The initial condition of the automaton is

$$I = CRUISE \times \{(x_r, y_r) \in \mathbb{R}^2 \mid 5^2 \leq x_r^2 + y_r^2 \leq r_a^2\} \tag{43}$$

where r_a is the radius of the alert zone. Thus the aircraft are assumed to be initially cruising and their protected zones do not intersect. The safety specification for H is that the state does not enter T, defined as

$$T = \{CRUISE, LEFT, STRAIGHT, RIGHT\} \times \{x_r^2 + y_r^2 \leq 5^2\} \tag{44}$$

Due to uncertainties in the velocity of the other aircraft, the worst case scenario is assumed for v_2 and therefore the dynamics evolve according to the saddle solution (42). This introduces additional switching surfaces within each discrete state.

The automaton of Figure 8 starts in the $CRUISE$ mode and flows in that state until the inter-aircraft distance is less than α_1 miles, at which point both aircraft make a heading change of $\Delta\phi$. Discrete heading changes have the effect of resetting the state by a rotation matrix since the coordinate frame depends on the orientation of the aircraft (6,7). In mode $LEFT$, both aircraft make a nominal lateral displacement of at least d. This is achieved using a timer variable t as shown. Both aircraft then return to their original heading and cruise until their relative distance is greater than α_2 miles. Once this is achieved, the reverse maneuver is performed in order return to the original cruise path and heading. The heading changes of both aircraft are assumed to occur simultaneously.

For this example, the velocities of the aircraft are chosen to be the same as in the second example of Section 3: $v_1 \in [2, 4]$, $v_2 = [1, 5]$ and $\phi_r = \pi/2$. The radius of the relative protected zone is 5 miles while the alert zone has a radius of 25 miles[1]. Instead of fixing values for the parameters d, α_1, α_2, and $\Delta\phi$, we initially leave the first three unrestricted, and let $\Delta\phi \in \{-45°, 45°\}$. Their values will be determined in order to minimize the unsafe set of initial states of the maneuver.

---

[1]The velocities and sizes of the zones are scaled in order to produce visualizable figures

CRUISE

Dynamics

$\dot{x}_r = -v_1 + v_2^* \cos(\phi_2 - \phi_1)$
$\dot{y}_r = v_2^* \sin(\phi_2 - \phi_1)$
$\dot{t} = 0$

Invariant

$x_r^2 + y_r^2 \geq \alpha_1$

LEFT

Dynamics

$\dot{x}_r = -v_1 + v_2^* \cos(\phi_2 - \phi_1)$
$\dot{y}_r = v_2^* \sin(\phi_2 - \phi_1)$
$\dot{t} = 1$

Invariant

$t \leq \max\left\{\dfrac{d}{\underline{v}_1 \sin \Delta\phi}, \dfrac{d}{\underline{v}_2 \sin \Delta\phi}\right\}$

$x_r^2 + y_r^2 < \alpha_1$

$\begin{bmatrix} x_r' \\ y_r' \end{bmatrix} = R(-\Delta\phi) \begin{bmatrix} x_r \\ y_r \end{bmatrix}$
$\phi_1' = \phi_1 + \Delta\phi$
$\phi_2' = \phi_2 + \Delta\phi$
$t' = 0$

$\begin{bmatrix} x_r' \\ y_r' \end{bmatrix} = R(-\Delta\phi) \begin{bmatrix} x_r \\ y_r \end{bmatrix}$
$\phi_1' = \phi_1 + \Delta\phi$
$\phi_2' = \phi_2 + \Delta\phi$
$t' = 0$

$t < 0$

$t > \max\left\{\dfrac{d}{\underline{v}_1 \sin \Delta\phi}, \dfrac{d}{\underline{v}_2 \sin \Delta\phi}\right\}$

$\begin{bmatrix} x_r' \\ y_r' \end{bmatrix} = R(\Delta\phi) \begin{bmatrix} x_r \\ y_r \end{bmatrix}$
$\phi_1' = \phi_1 - \Delta\phi$
$\phi_2' = \phi_2 - \Delta\phi$
$t' = t$

RIGHT

Dynamics

$\dot{x}_r = -v_1 + v_2^* \cos(\phi_2 - \phi_1)$
$\dot{y}_r = v_2^* \sin(\phi_2 - \phi_1)$
$\dot{t} = -1$

Invariant

$t \geq 0$

$\begin{bmatrix} x_r' \\ y_r' \end{bmatrix} = R(\Delta\phi) \begin{bmatrix} x_r \\ y_r \end{bmatrix}$
$\phi_1' = \phi_1 - \Delta\phi$
$\phi_2' = \phi_2 - \Delta\phi$
$t' = t$

STRAIGHT

Dynamics

$\dot{x}_r = -v_1 + v_2^* \cos(\phi_2 - \phi_1)$
$\dot{y}_r = v_2^* \sin(\phi_2 - \phi_1)$
$\dot{t} = 0$

Invariant

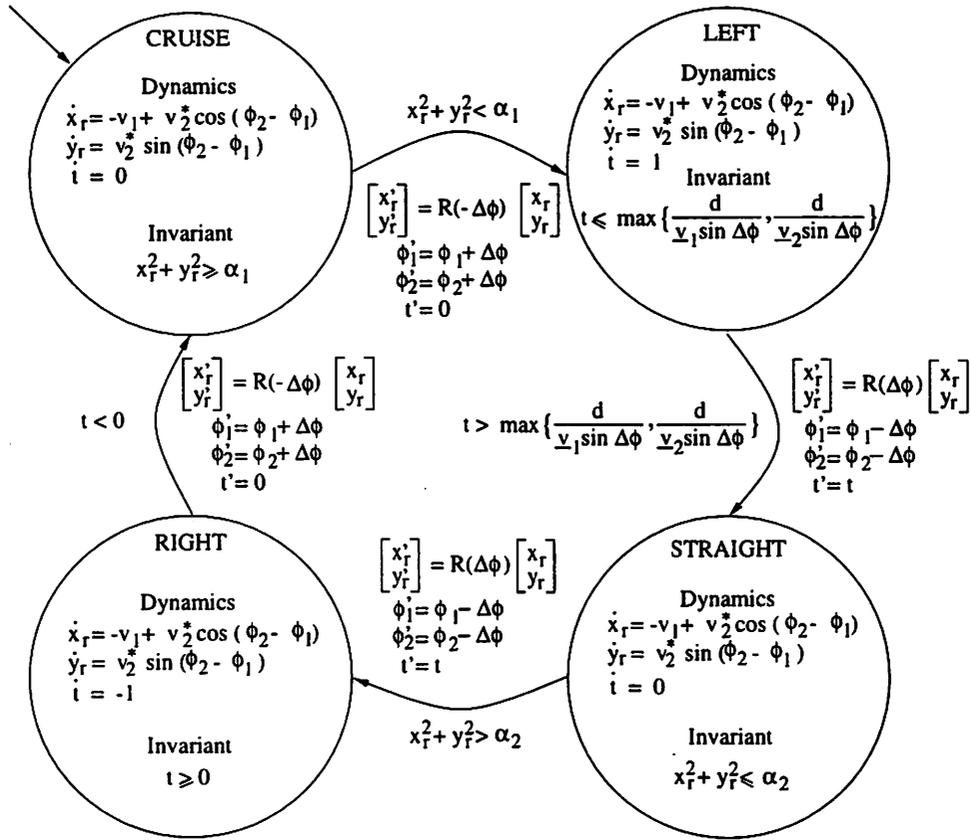$x_r^2 + y_r^2 \leq \alpha_2$

$x_r^2 + y_r^2 > \alpha_2$

Figure 8: Modeling conflict resolution maneuver as a hybrid automaton
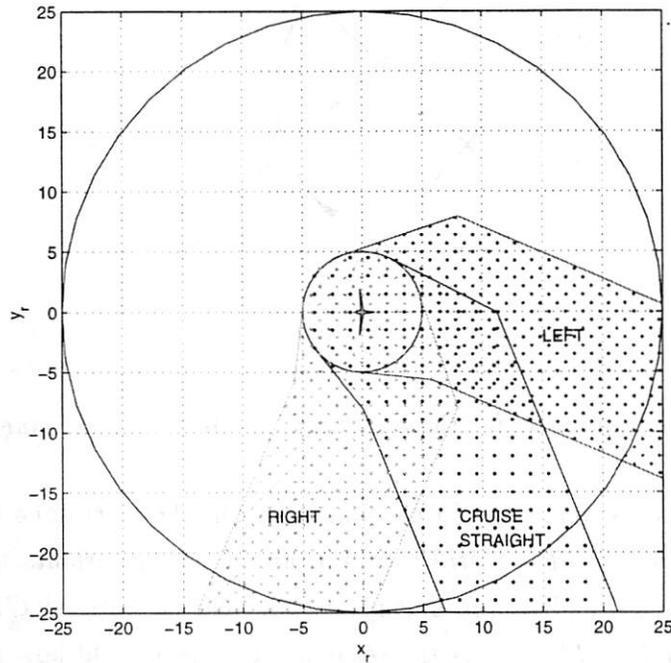
Figure 9: Computation of $Pre_{-\infty}(T)$ for each discrete state in $\{CRUISE, LEFT, STRAIGHT, RIGHT\}$.
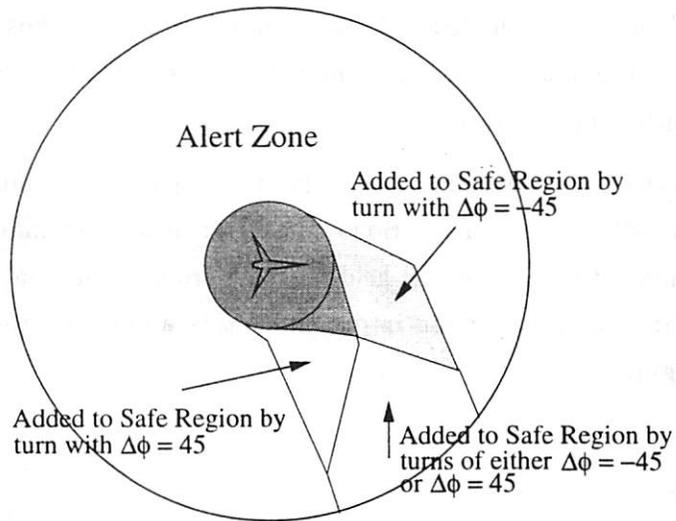

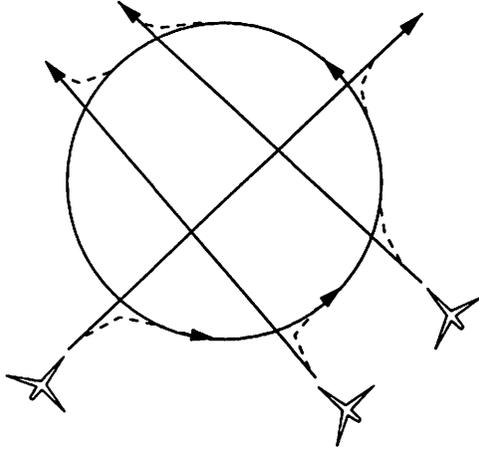Figure 10: Partitioning the Alert Zone into safe and unsafe regions

Figure 11: Conflict Resolution for three aircraft: the Roundabout maneuver

Figure 9 displays the union of each $Pre_{-\infty}(T)$ calculated within the alert zone for each discrete state ($CRUISE, LEFT, STRAIGHT, RIGHT$), in the absence of invariants for each discrete state since the parameters d, α_1, and α_2 are unconstrained. The set labeled $CRUISE$ (respectively $LEFT, STRAIGHT, RIGHT$) displays the set of states which could flow into T under the $CRUISE$ mode (respectively $LEFT, STRAIGHT, RIGHT$ modes). $Pre_{-\infty}(T)$ in the $LEFT$ and $RIGHT$ modes are rotations of this set in the $CRUISE$ mode by $-\Delta\phi$, corresponding to aircraft 1 at the origin of the relative frame rotating by $\Delta\phi$. The intersection of the sets $Pre_{-\infty}(T)$ in this figure represents those states which are unsafe under *all* modes, since outside of this intersection the aircraft may always switch modes to enter a safe region, by choosing appropriate values for the parameters d, α_1, α_2. Figure 10 displays the minimal unsafe set as a subset of the $Pre_{-\infty}(T)$ in the $CRUISE$ maneuver (shown as the shaded set). For values of d, α_1, α_2, chosen so that the switches between modes occurs on the boundary of this minimal set, the iterative computation (13) reaches a fixed point $Pre^*(T)$ after three iterations.

The type of maneuver that may be verified with this technique can be much more general than that described here: in [45] we construct various parameter-dependent maneuvers for two, three, and four aircraft by using artificial potential field methods from robotic path planning to produce the maneuvers. For three aircraft coming into conflict this approach produces the *Roundabout* maneuver, shown in Figure 11.

5   Conclusions

In this paper, we have presented a methodology for generating provably safe conflict resolution maneuvers for two aircraft. The method is based on calculating reachable sets for hybrid systems

with nonlinear dynamics within each discrete state. The approach allows for uncertainty in the intent of one of the aircraft, and calculates the least restrictive control scheme for the other aircraft, based on the worst case uncertainty. This calculation is then used to determine, for a given maneuver with possible variation in its parameters, the minimal unsafe operating region for each aircraft.

Important research issues that we are currently addressing are the computation of numerical solutions to the Hamilton-Jacobi-Isaacs partial differential equation and the efficient representation and manipulation of $Pre^*(T)$. The computation of the solution to the Hamilton-Jacobi-Isaacs PDE when $J^*(x, t)$ is *not* a smooth function of x and t is possible, a survey paper [46] presents efficient computation schemes. In addition, we are extending the verification methodology to include lift and drag aerodynamic forces in the dynamics of the aircraft. Some preliminary results in this context have been presented in [25], [43]. Finally, we are investigating *probabilistic verification*, which calculates the probability of a system trajectory entering an unsafe region.

6 Appendix

Proof of Proposition 1: Starting at time t (free) and integrating to the final time 0, the solution to equations (39) has $\phi_r(t) = \phi_r(0)$ and

$$
\begin{aligned}
x_r(0) &= x_r(t) - \int_t^0 u(\tau)d\tau + \cos\phi_r \; \int_t^0 d(\tau)d\tau \\
y_r(0) &= y_r(t) + \sin\phi_r \int_t^0 d(\tau)d\tau
\end{aligned}
\tag{45}
$$

Substituting equations (45) into the cost index (15), (30), and ignoring the constant 5^2 results in

$$
\begin{aligned}
J(x, u(\cdot), d(\cdot), t) &= x_r^2(0) + y_r^2(0) \\
&= x_r^2(t) + y_r^2(t) - x_r(t)\int_t^0 u(\tau)d\tau - x_r(0)\int_t^0 u(\tau)d\tau \\
&\quad + \int_t^0 d(\tau)d\tau[x_r(t)\cos\phi_r + y_r(t)\sin\phi_r] + \int_t^0 d(\tau)d\tau[x_r(0)\cos\phi_r + y_r(0)\sin\phi_r]
\end{aligned}
$$

Define the *switching functions* $s_1(t), s_2(t)$ as in equations (40). Consider the case in which, $\forall t \le 0$,

$$
sgn(s_1(t)) > 0, \quad sgn(s_2(t)) > 0
$$

We will show that in this case the saddle solution is $u^* = \underline{v}_1$ and $d^* = \underline{v}_2$. Note that we assume that in the interval $[t, 0]$, both $s_1(t)$ and $s_2(t)$ *do not change sign*. If t is such that the switching functions do change sign on this interval, then the interval must be broken into two intervals, and the saddle solution calculated separately for each interval.

Let $d = d^*$ and vary u, ie. let $u = \underline{v}_1 + \delta v_1$, where $\delta v_1 \ge 0$. Then

$$
J(x, u(\cdot), d^*(\cdot), t) = x_r^2(t) + y_r^2(t) - x_r(t)\underline{v}_1(0 - t) - x_r(0)\underline{v}_1(0 - t)
$$

23

$$-x_r(t) \int_t^0 \delta v_1(\tau) d\tau - x_r(0) \int_t^0 \delta v_1(\tau) d\tau$$

$$+\underline{v}_2(0-t)[x_r(t)\cos\phi_r + y_r(t)\sin\phi_r] + \underline{v}_2(0-t)[x_r(0)\cos\phi_r + y_r(0)\sin\phi_r]$$

$$\leq \quad x_r^2(t) + y_r^2(t) - x_r(t)\underline{v}_1(0-t) - x_r(0)\underline{v}_1(0-t)$$

$$+\underline{v}_2(0-t)[x_r(t)\cos\phi_r + y_r(t)\sin\phi_r] + \underline{v}_2(0-t)[x_r(0)\cos\phi_r + y_r(0)\sin\phi_r]$$

$$= \quad J(x, u^*(\cdot), d^*(\cdot), t) \tag{46}$$

Similarly, let $u = u^*$ and vary d, ie. let $d = \underline{v}_2 + \delta v_2$, where $\delta v_2 \geq 0$. Then

$$J(x, u^*(\cdot), d(\cdot), t) = x_r^2(t) + y_r^2(t) - x_r(t)\underline{v}_1(0-t) - x_r(0)\underline{v}_1(0-t)$$

$$+\underline{v}_2(0-t)[x_r(t)\cos\phi_r + y_r(t)\sin\phi_r] + \underline{v}_2(0-t)[x_r(0)\cos\phi_r + y_r(0)\sin\phi_r]$$

$$+ \int_t^0 \delta v_2(\tau) d\tau [x_r(t)\cos\phi_r + y_r(t)\sin\phi_r]$$

$$+ \int_t^0 \delta v_2(\tau) d\tau [x_r(0)\cos\phi_r + y_r(0)\sin\phi_r]$$

$$\geq \quad x_r^2(t) + y_r^2(t) - x_r(t)\underline{v}_1(0-t) - x_r(0)\underline{v}_1(0-t)$$

$$+\underline{v}_2(0-t)[x_r(t)\cos\phi_r + y_r(t)\sin\phi_r] + \underline{v}_2(0-t)[x_r(0)\cos\phi_r + y_r(0)\sin\phi_r]$$

$$= \quad J(x, u^*(\cdot), d^*(\cdot), t) \tag{47}$$

Summarizing, we have shown above that in this case,

$$J(x, u(\cdot), d^*(\cdot), t) \leq J(x, u^*(\cdot), d^*(\cdot), t) \leq J(x, u^*(\cdot), d(\cdot), t) \tag{48}$$

Therefore, $u^* = \underline{v}_1$, $d^* = \underline{v}_2$ is a saddle solution in this case. The three other cases can be shown in a similar manner. $\square$

References

[1] Honeywell Inc. Markets Report. Technical Report NASA Contract NAS2-114279, Final Report for AATT Contract, 1996.

[2] T. S. Perry. In search of the future of air traffic control. *IEEE Spectrum*, 34(8):18–35, 1997.

[3] Radio Technical Commission for Aeronautics. Final report of RTCA Task Force 3: Free flight implementation. Technical report, RTCA, Washington DC, October 1995.

[4] Honeywell Inc. Technology and Procedures Report. Technical Report NASA NAS2-114279, Final Report for AATT Contract, 1996.

[5] Honeywell Inc. Concepts and Air Transportation Systems Report. Technical Report NASA Contract NAS2-114279, Final Report for AATT Contract, 1996.

[6] W. H. Harman. TCAS : A system for preventing midair collisions. *The Lincoln Laboratory Journal*, 2(3):437–457, 1989.

[7] H. Erzberger, T. J. Davis, and S. Green. Design of Center-TRACON Automation System. In *Proceedings of the AGARD Guidance and Control Syposium on Machine Intelligence in Air Traffic Management*, pages 11.1–11.12, Berlin, Germany, 1993.

[8] D. J. Brudnicki and A. L. McFarland. User Request Evaluation Tool (URET) conflict probe performance and benefits assessment. In *Proceedings of the U.S.A./Europe ATM Seminar*, Eurocontrol, Paris, 1997.

[9] L. Yang and J. Kuchar. Prototype conflict alerting logic for free flight. In *Proceedings of the 35th AIAA Aerospace Sciences Meeting & Exhibit, AIAA 97-0220*, Reno, NV, January 1997.

[10] R. A. Paielli and H. Erzberger. Conflict probability and estimation for free flight. In *Proceedings of the 35th AIAA Aerospace Sciences Meeting & Exhibit, AIAA 97-0001*, Reno, NV, January 1997.

[11] J. Krozel, T. Mueller, and G. Hunter. Free flight conflict detection and resolution analysis. In *Proceedings of the AIAA Guidance, Navigation and Control Conference, AIAA-96-3763*, San Diego, CA, August 1996.

[12] Y. Zhao and R. Schultz. Deterministic resolution of two aircraft conflict in free flight. In *Proceedings of the AIAA Guidance, Navigation and Control Conference, AIAA-97-3547*, New Orleans, LA, August 1997.

[13] J.-H. Oh and E. Feron. Fast detection and resolution of multiple conflicts for 3-Dimensional free flight. In *Proceedings of the IEEE Conference on Decision and Control*, San Diego, CA, 1997.

[14] R. Slattery and S. Green. Conflict free trajectory planning for air traffic control automation. Technical Report NASA TM-108790, NASA Ames Research Center, Moffett Field, CA, January 1994.

[15] C. Tomlin, G. Pappas, J. Lygeros, D. Godbole, and S. Sastry. Hybrid control models of next generation Air Traffic Management. In P. Antsaklis, W. Kohn, A. Nerode, and S. Sastry, editors, *Hybrid Systems IV*, Lecture Notes in Computer Science 1273, pages 378–404. Springer-Verlag, 1997. Longer version available as UCB/ERL Memo M97/7.

[16] Robert L. Grossman, Anil Nerode, Anders P. Ravn, and Hans Rischel, editors. *Hybrid Systems*. Lecture Notes in Computer Science 736. Springer-Verlag, 1993.

[17] Panos Antsaklis, Wolf Kohn, Anil Nerode, and Shankar Sastry, editors. *Hybrid Systems II*. Lecture Notes in Computer Science 999. Springer-Verlag, 1995.

[18] R. Alur, T.A. Henzinger, and E.D. Sontag, editors. *Hybrid Systems III*. Lecture Notes in Computer Science 1066. Springer-Verlag, 1996.

[19] P Antsaklis, W. Kohn, A. Nerode, and S. Sastry, editors. *Hybrid Systems IV*. Lecture Notes in Computer Science 1273. Springer-Verlag, 1997.

[20] Rajeev Alur and David Dill. A theory of timed automata. *Theoretical Computer Science*, 126:183–235, 1994.

[21] R. Alur, C. Courcoubetis, T.A. Henzinger, P.-H. Ho, X. Nicollin, A. Olivero, J. Sifakis, and S. Yovine. The algorithmic analysis of hybrid systems. In G. Cohen and J.-P. Quadrat, editors, *Proceedings of the 11th International Conference on Analysis and Optimization of Systems: Discrete-event Systems*, Lecture Notes in Control and Information Sciences 199, pages 331–351. Springer-Verlag, 1994.

[22] N. Lynch, R. Segala, F. Vaandrager, and H.B. Weinberg. Hybrid I/O automata. In *Hybrid Systems III*, Lecture Notes in Computer Science 1066, pages 496–510. Springer-Verlag, 1996.

[23] T.A. Henzinger. The theory of hybrid automata. In *Proceedings of the 11th Annual Symposium on Logic in Computer Science*, pages 278–292. IEEE Computer Society Press, 1996.

[24] A. Puri and P. Varaiya. Decidability of of hybrid systems with rectangular differential inclusions. In *Proceedings of the 6th International Computer Aided Verification Conference, Stanford, CA*, pages 95–104, 1994.

[25] G. Pappas and S. Sastry. Towards continuous abstractions of dynamical and control systems. In P. Antsaklis, W. Kohn, A. Nerode, and S. Sastry, editors, *Hybrid Systems IV*, Lecture Notes in Computer Science 1273, pages 329–341. Springer-Verlag, New York, 1997.

[26] Z. Manna and A. Pnueli. *Temporal Verification of Reactive Systems: Safety*. Springer-Verlag, New York, 1995.

[27] O. Maler, A. Pnueli, and J. Sifakis. On the synthesis of discrete controllers for timed systems. In Ernst W. Mayr and Claude Puech, editors, *STACS 95: Theoretical Aspects of Computer Science*, Lecture Notes in Computer Science 900, pages 229–242. Springer Verlag, Munich, 1995.

[28] H. Wong-Toi. The synthesis of controllers for linear hybrid automata. In *Proceedings of the IEEE Conference on Decision and Control*, San Diego, CA, 1997.

[29] T. A. Henzinger, P. H. Ho, and H. Wong-Toi. A user guide to HYTECH. In E. Brinksma, W. Cleaveland, K. Larsen, T. Margaria, and B. Steffen, editors, *TACAS 95: Tools and Algorithms for the Construction and Analysis of Systems*, Lecture Notes in Computer Science 1019, pages 41–71. Springer Verlag, 1995.

[30] C. Daws, A. Olivero, S. Tripakis, and S. Yovine. The tool KRONOS. In *Hybrid Systems III, Verification and Control*, pages 208–219. Lecture Notes in Computer Science 1066, Springer-Verlag, 1996.

[31] N. Bjorner, A. Browne, E. Chang, M. Colon, A. Kapur, Z. Manna, H. Sipma, and T. Uribe. STeP: The Stanford Temporal Prover (educational release), user's manual. Technical report, STAN-CS-TR-95-1562, Department of Computer Science, Stanford University, 1995.

[32] R.W. Brockett. Hybrid models for motion control systems. In H. Trentelman and J.C. Willems, editors, *Perspectives in Control*, pages 29–54. Birkhauser, Boston, 1993.

[33] M. S. Branicky. *Control of Hybrid Systems*. PhD thesis, Department of Electrical Engineering and Computer Sciences, Massachusetts Institute of Technology, 1994.

[34] L. Tavernini. Differential automata and their discrete simulators. *Nonlinear Analysis, Theory, Methods and Applications*, 11(6):665–683, 1987.

[35] A. Deshpande. *Control of Hybrid Systems*. PhD thesis, Department of Electrical Engineering and Computer Sciences, University of California at Berkeley, 1994.

[36] J. Lygeros. *Hierarchical, Hybrid Control of Large Scale Systems*. PhD thesis, Department of Electrical Engineering and Computer Sciences, University of California at Berkeley, 1996.

[37] A. Nerode and W. Kohn. Models for hybrid systems: Automata, topologies, controllability, observability. In Robert L. Grossman, Anil Nerode, Anders P. Ravn, and Hans Rischel, editors, *Hybrid System*, Lecture Notes in Computer Science 736, pages 317–356. Springer Verlag, New York, 1993.

[38] M. Lemmon, J. A. Stiver, and P. J. Antsaklis. Event identification and intelligent hybrid control. In Robert L. Grossman, Anil Nerode, Anders P. Ravn, and Hans Rischel, editors, *Hybrid Systems*, Lecture Notes in Computer Science 736, pages 268–296. Springer Verlag, New York, 1993.

[39] M. Heymann, F. Lin, and G. Meyer. Control synthesis for a class of hybrid systems subject to configuration-based safety constraints. In O. Maler, editor, *Hybrid and Real Time Systems*, Lecture Notes in Computer Science 1201, pages 376–391. Springer Verlag, 1997.

[40] R. Isaacs. *Differential Games*. John Wiley, 1967.

[41] T. Başar and G. J. Olsder. *Dynamic Non-cooperative Game Theory*. Academic Press, second edition, 1995.

[42] J. Lygeros, D. N. Godbole, and S. Sastry. A verified hybrid controller for automated vehicles. Technical Report UCB-ITS-PRR-97-9, Institute of Transportation Studies, University of California, Berkeley, 1997. To appear in the IEEE Transactions on Automatic Control, Special Issue on Hybrid Systems, April 1998.

[43] J. Lygeros, C. Tomlin, and S. Sastry. Multiobjective hybrid controller synthesis. In O. Maler, editor, *Hybrid and Real-Time Systems*, Lecture Notes in Computer Science 1201, pages 109–123. Springer-Verlag, Grenoble, 1997.

[44] C. Tomlin, G. Pappas, and S. Sastry. Conflict resolution for air traffic management: A case study in multi-agent hybrid systems. Technical report, UCB/ERL M96/38, Electronics Research Laboratory, University of California, Berkeley, 1996.

[45] J. Košecká, C. Tomlin, G. Pappas, and S. Sastry. Generation of conflict resolution maneuvers for air traffic management. In *International Conference on Intelligent Robots and Systems (IROS)*, pages 1598–1603, Grenoble, 1997.

[46] J. A. Sethian. Theory, algorithms, and applications of level set methods for propagating interfaces. Technical report, Center for Pure and Applied Mathematics (PAM-651), University of California, Berkeley, 1995.